Enhancement LVRT capability of DFIG driven wind conversion system

Abdeslam Jabal Laafou[1], Abdessalam Ait Madi[1], Youssef Moumani[1], Hassan Essakhi[2]
[1]Laboratory of Advanced Systems Engineering, Ibn Tofail University, Kenitra, Morocco
[2]Laboratory of Engineering Sciences and Energy Management, Higher School of Technology, Ibn Zohr University, Agadir, Morocco

| Article Info	ABSTRACTs
Article history: Received Apr 29, 2024 Revised Sep 2, 2024 Accepted Oct 23, 2024 *Keywords:* Crowbar DFIG LVRT SDBR Voltage dip Wind turbine	In this paper we present two techniques for protecting the doubly fed induction generator (DFIG) in the event of external disturbances on the electrical network, the crowbar circuit and series dynamic braking resistor (SDBR) techniques. During voltage dips, the first technique is triggered and short-circuits the rotor side converter (RSC) so as to maintain the rotor current within the desired limits. As a result, the DFIG behaves as an asynchronous cage generator that absorbs the reactive power coming from the voltage dip on the network which does not meet the grid code's (GC) requirements. The second technique makes it possible to limit overcurrent's at the level of the stator and rotor of the DFIG, it will enable the wind power system to continue operating normally once the fault has disappeared and to stay connected to the network throughout the voltage dip. This SDBR technique presents a good compromise between its performance, its simplicity, its efficiency, and its implementation's cost.
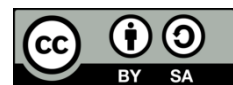
Corresponding Author:

Abdeslam Jabal Laafou
Laboratory of Advanced Systems Engineering, Ibn Tofail University
Kenitra, Morocco
Email: abdeslam.jaballaafou@uit.ac.ma

1. INTRODUCTION

The significant focus on renewable energy sources, particularly wind energy, has led to an increase in installed wind capacity within electrical grids [1]. Due to this high penetration of wind energy in the grid, it must address challenges to ensure stability. Consequently, grid codes require wind energy systems to participate more actively in maintaining the operability and quality of the electrical grid [2].

Wind energy systems based on the doubly-fed induction generator (DFIG) have been widely used due to their advantages. However, because of the direct connection between the DFIG stator and the grid, a voltage dip causes the voltage at the DFIG terminals to drop significantly, resulting in very high currents flowing through the stator and rotor windings [3], [4]. This affects the normal operation of the DFIG and can lead to its destruction along with its converters. Previously, to protect against such faults, wind turbines were allowed to disconnect from the electrical grid. However, this approach was not beneficial for either the producer or the grid operator, as the disconnection of a wind farm with hundreds of megawatts could disrupt the grid and prolong the time required to restore the nominal voltage. Therefore, grid operators were compelled to update the standards and requirements of the grid codes [2]. Today, wind turbines are no longer permitted to disconnect during voltage dips and must contribute to voltage recovery by injecting reactive power [5]. Indeed, wind turbines are now required to behave as closely as possible to conventional power plants.

To ensure that the wind turbine remains connected to the grid during voltage dips, the DFIG must comply with grid code requirements. Various protective approaches have been proposed and documented in the literature. These approaches can be broadly classified into two main categories [2], [6], [7] the first category involves improving control schemes (software solutions), while the second category involves hardware solutions (adding auxiliary equipment). Among the control strategies developed by researchers, notable examples include modified vector control [8], transient current control with predictive actions [9], and predictive control models [10]. These solutions can limit fault currents in the case of minor voltage dips. However, they are less effective in severe voltage dips, where they cannot limit fault currents sufficiently to ensure safe operation [2]. Therefore, hardware approaches are necessary to meet grid code requirements and limit overcurrent's during significant voltage dips. Among the hardware solutions used to protect the DFIG from overcurrent's, the "crowbar" protection system is widely used in wind applications. This protection device consists of a crowbar circuit combined with a DC-chopper circuit to limit high currents and voltages. But during the hollow tension the crowbar short-circuits the converter rotor side converter (RSC) to maintain the current of the rotor in the prescript limits. As a result, the DFIG behaves like an asynchronous cage generator. This does not meet grid codes standards as it absorbs the reactive power from the grid's voltage dip.

In this paper, we first study the DFIG's response in the case of a voltage dip. Then we will propose two methods of protecting the wind turbine (WT) against overcurrent's. The first is based on the crowbar protection circuit and the second method is based on the SDBR in series with the stator to overcome the disadvantages of the first technique and finally, we will make a comparison between these two methods.

2.   THE OPERATION OF THE DFIG UNDER A SYMMETRIC VOLTAGE DIP

According to the EN 50160 standard, a voltage dip is defined as a sudden drop in voltage, between 10% and 90% of the nominal effective value, at a point in the electrical grid for a duration of between 10 ms and 1 min [11]. It is said to be symmetrical when the voltage drop is constant on the three phases. This type of malfunction [12] is due to a short circuit between the three phases and ground or a high current demand during the startup of a high-power motor.

Assuming proper operation of the DFIG, a symmetrical voltage sag of depth d occurs on the grid at instant t_0. The (1) and (2) can be used to rewrite the voltage and forced stator flux, respectively [13]-[16].

$$\underline{V_s} = \begin{cases} V_s e^{j\omega_s t} & , \quad si \ t < t_0 \\ (1-d)V_s e^{j\omega_s t} & , \quad si \ t \geq t_0 \end{cases} \tag{1}$$

$$\underline{\psi_{sf}} = \begin{cases} \dfrac{V_s}{j\omega_s} e^{j\omega_s t} & , \quad si \ t < t_0 \\ (1-d)\dfrac{V_s}{j\omega_s} e^{j\omega_s t} & , \quad si \ t \geq t_0 \end{cases} \tag{2}$$

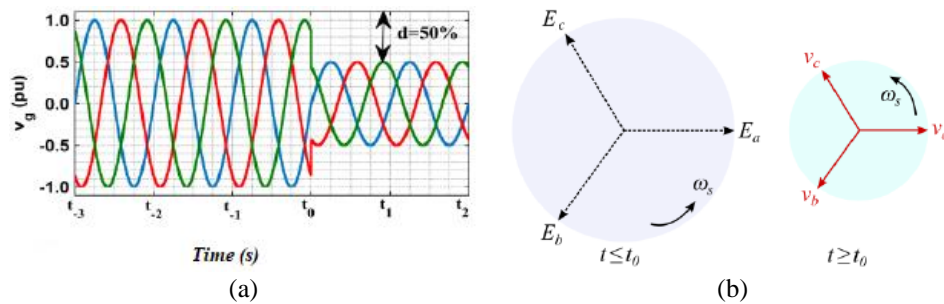A voltage sag example with a depth of d = 50% is shown in Figure 1.

Figure 1. Voltage dip representation: (a) voltage dip with a depth of 50% and (b) voltage dip signature

2.1. DFIG rotor operating in open circuit

For an open-circuit rotor, the differential equation representing the flux's evolution is given by (3).

$$\frac{d\psi_s(t)}{dt} + \frac{R_s}{L_s}\psi_s(t) = v_s(t) \tag{3}$$

Once this differential equation is solved, (4) becomes the new expression for the stator flux [17].

$$\underline{\psi}_s(t \geq t_0) = \underbrace{(1-d)\frac{V_s}{j\omega_s}e^{j\omega_s t}}_{\underline{\psi}_{sf}} + \underbrace{d\frac{V_s}{j\omega_s}e^{-\frac{t}{\tau_s}}}_{\underline{\psi}_{sn}} \tag{4}$$

Where $\tau_s = \frac{L_s}{R_s}$: is the stator windings constant time.

The expression of the preceding flux consists of two terms:

- The first term $\underline{\psi}_{sf}$ corresponds to the forced flux during the voltage sag, imposed by the electrical grid.
- The second term $\underline{\psi}_{sn}$ refers to the natural flux in the DFIG which is dependent on initial conditions (the magnetic state of the generator, the depth d of the voltage sag). This flux decreases exponentially with a time-constant $\frac{1}{\tau_s}$ ensuring that no discontinuity appears in the magnetic state of the DFIG during the fault.

Figure 2 illustrates the evolution of the two flux terms: the forced flux $\underline{\psi}_{sf}$ and the natural flux $\underline{\psi}_{sn}$. During the voltage sag, the forced flux vector continues to rotate at the speed of ω_s, while the natural flux vector does not rotate and exponentially decays until it disappears after the voltage sag.
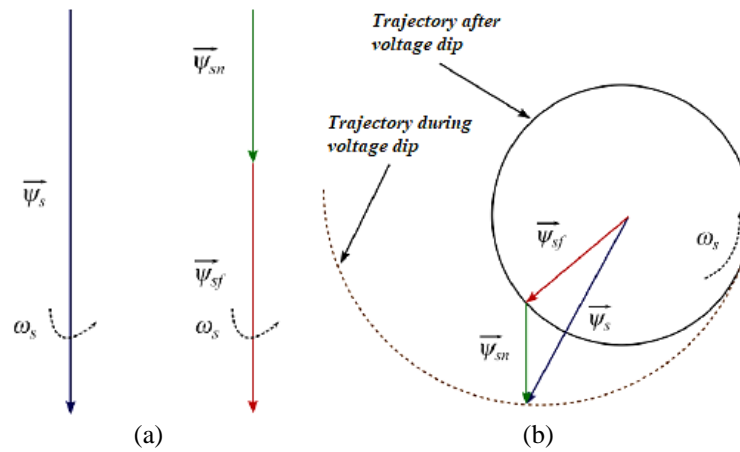

Figure 2. Vector representation of the stator flux at the beginning of the voltage dip:
(a) at the start of voltage dip and (b) during voltage dip

Each term of the stator flux induces its own component for the open-circuit rotor voltage. The rotor voltage $\underline{V}_{r0}$ is composed of two terms: the first term $\underline{V}_{rf}$ is deduced from the forced flux, and the second term $\underline{V}_{rn}$ is deduced from the natural flux. Therefore, can be expressed as (5).

$$\underline{V}_{r0} = \underline{V}_{rf} + \underline{V}_{rn} \tag{5}$$

By substituting (4) into (5), the new expression for the voltage $\underline{V}_{r0}$ will be given by (6).

$$\underline{V}_{r0} = \frac{L_m}{L_s}(1-d)gV_s e^{j\omega_s t} - \frac{L_m}{L_s}\left(\frac{1}{\tau_s}+j\omega\right)d\frac{V_s}{j\omega_s}e^{-\frac{t}{\tau_s}} \tag{6}$$

Neglecting the term $\frac{1}{\tau_s}$, $\underline{V}_{r0}$ mentioned earlier will be expressed by (7) [18], [19].

$$\underline{V}_{r0} = \underbrace{\frac{L_m}{L_s}(1-d)gV_s e^{j\omega_s t}}_{V_{rf}} - \underbrace{\frac{L_m}{L_s}d\frac{\omega}{\omega_s}V_s e^{-\frac{t}{\tau_s}}}_{V_{rn}} \tag{7}$$

The voltage V_{rf} which is caused by the forced stator flux $\underline{\psi}_{sf}$, its maximum value can be expressed by (8).

$$V_{rf-max} = \frac{L_m}{L_s}(1 - d)|g|V_s \tag{8}$$

$\underline{V_{rn}}$ is the voltage induced in the rotor by the natural stator flux $\underline{\psi_{sn}}$. It is proportional to the depth d of the voltage sag. At the moment of the voltage sag occurrence ($t = t_0$), the amplitude of this component can reach its maximum value described by (9).

$$V_{rn-max} = \frac{L_m}{L_s}(1 - g)dV_s \tag{9}$$

2.2. DFIG rotor operation while connected to the RSC

As mentioned earlier and considering that the rotor resistance R_r and the transient inductance of the rotor σL_r have low values, the rotor voltage in the absence of the RSC (open circuit) does not differ significantly from the rotor voltage in the presence of the RSC when the power converter RSC is connected to the rotor. Similarly, for the voltage $\underline{V_r}$ and during the voltage sag, the rotor current $\underline{I_r}$ is the sum of the forced current $\underline{I_{rf}}$ due to the voltage $\underline{V_{rf}}$ and the transient current produced by the voltage $\underline{V_{rn}}$.

$$\underline{I_r} = \underline{I_{rf}} + \underline{I_{rn}} \tag{10}$$

From (10), in cases where the depth of the voltage sag is more significant, any increase in rotor voltage leads to an undesirable increase in current in the rotor windings of the machine and in the RSC. Therefore, to protect the RSC against undesirable overcurrent's due to the voltage sag, it is essential to effectively control the RSC by applying reliable and robust techniques to limit this high current.

3. METHOD

3.1. Protection using active circuits (crowbar)

Current limitation circuits (crowbars) are dedicated to restricting excessive currents caused by voltage sags. These circuits can take various forms and are generally placed between the rotor and the RSC, as indicated in Figure 3, to limit the current in the latter [20], [21]. Most of these structures use fast-switching controlled switches such as insulated-gate bipolar transistor (IGBT) transistors to trigger after the occurrence of voltage sags in the grid, dissipating the excess power in the dissipation resistance. The primary disadvantage of crowbar circuits is that, upon crowbar activation, the RSC deactivates, rendering the DFIG uncontrollable. As a result, the DFIG functions similarly to a squirrel cage induction machine (SCIM) but with a higher rotor resistance. The DFIG absorbs a significant amount of reactive power in such a scenario to maintain its magnetization state at the required level. This results in further degradation of the grid voltage and extends the recovery time [3].

A voltage limiting circuit at the DC bus level using a controlled IGBT transistor and a dissipative resistor mounted in parallel with the DC bus can also be considered, as illustrated in Figure 3. This structure helps to maintain the DC bus voltage within an operational range around its nominal value. In Figure 3, the diodes and the IGBT transistor are assumed to be ideal; thus, the voltage across the resistor R_{cw} is defined by the relationship expressed in (11) [22].

$$v_{cw} = S_{cw}I_{cw}R_{cw} \tag{11}$$

In order to control the switch T_{cw}, the control circuit develops the function S_{cw}: $S_{cw} = 0$ if T_{cw} is open $S_{cw} = 1$ if T_{cw} is closed

The protective circuit's control strategy using a crowbar is shown in Figure 4. When any of the rotor currents surpass the safety current I_{r-sct}, the crowbar circuit is activated; otherwise, it remains disconnected. The control signal for the IGBT switches is based on hysteresis comparators.

In this instance, the switch modifies the DFIG model by triggering the crowbar in response to the voltage sag and connecting the dissipation resistor R_{cw} in series with the rotor windings. In order to maintain a steady DC bus voltage, the grid side converter (GSC) stays connected to the grid while the RSC is simultaneously unplugged from the DFIG. The updated DFIG model is shown in Figure 5 during a voltage sag. According to Figure 5, we can say that the value of the crowbar resistance R_{cw} influences the overall model of the DFIG. If the value of the resistance R_{cw} is reduced, there will be an increase in the electromagnetic torque and rotor current overloads. Conversely, a high value of the resistance R_{cw} leads to reduced rotor currents and electromagnetic torque, and higher values of rotor voltages. Therefore, it is crucial

to carefully choose the value of the resistance R_{cw} to avoid these constraints. It should be noted that the value of the resistance R_{cw} is much larger than the resistance of the rotor and stator [17], [23], [24].
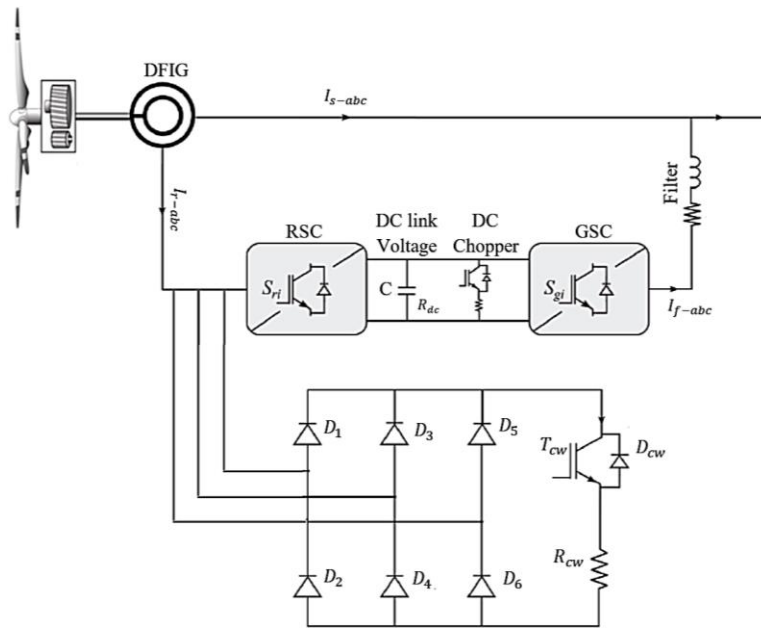

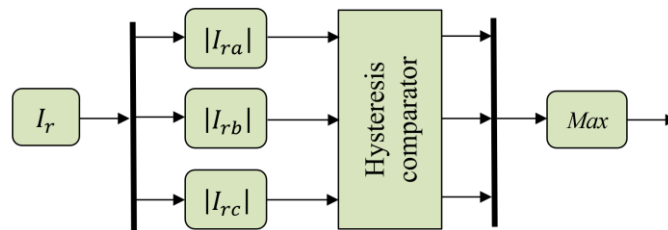Figure 3. Active current limitation (crowbar) and DC bus voltage (DC chopper) circuit

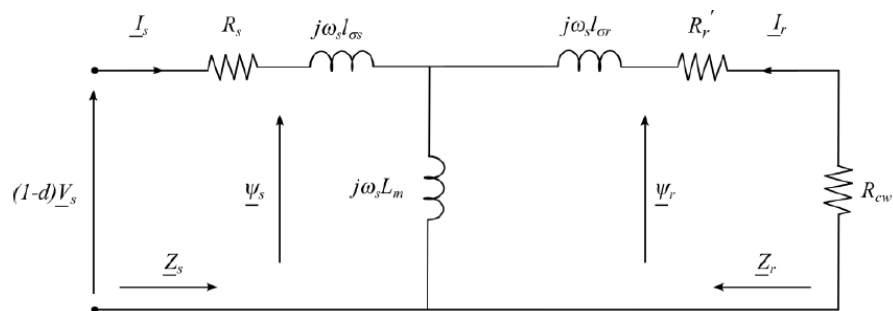Figure 4. Control scheme of the crowbar circuit

Figure 5. Model of the DFIG during a voltage sag with crowbar

3.2. Protection of series dynamic braking resistor

The series dynamic braking resistor (SDBR) device is based on a resistor in parallel with an IGBT switch, as shown in Figure 6. This device is connected in series with the stator to limit the induced overvoltage from the transient stator flux, thereby reducing the current in the rotor and limiting the DC bus voltage during a voltage sag [2], [25].

The control block of the SDBR is depicted in Figure 7. Under normal conditions, the control block sends a signal of 1 to the IGBT switch, allowing it to be closed, and the braking resistor is short-circuited, playing no role. In the event of a voltage sag, the control block sends a signal of 0 to the IGBT switch, causing it to open, and the braking resistor is then connected in series with the stator. The resistor remains connected until the stator voltage returns to its normal value, at which point the IGBT switch returns to its normal state (closed) [26], [27].
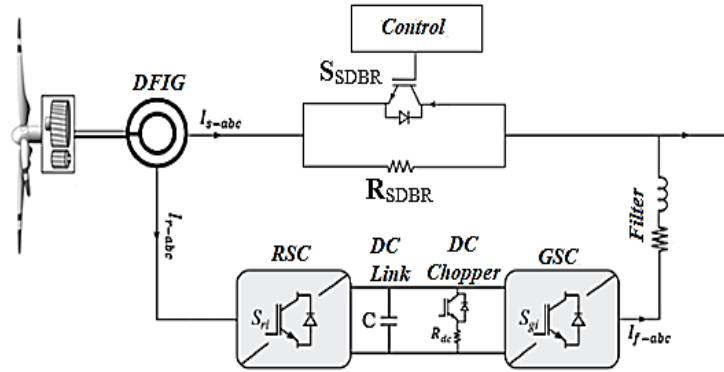
Figure 6. Block diagram for the SDBR technique
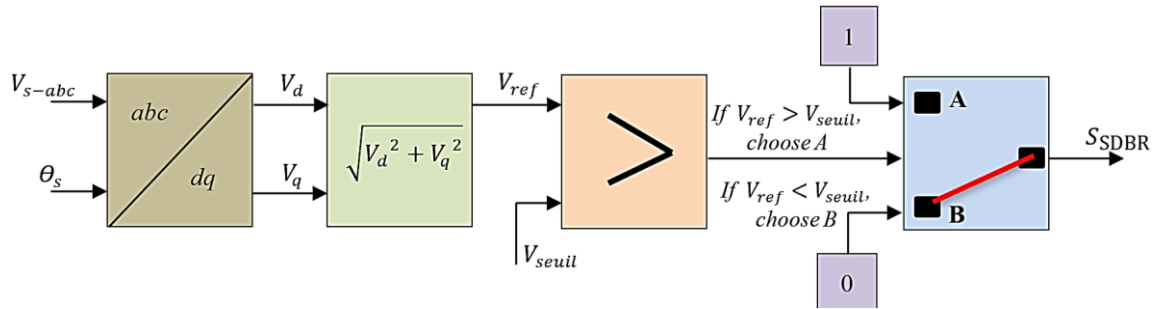
Figure 7. Control scheme for the SDBR technique

As in the crowbar circuit, the resistance in the SDBR technique must be chosen considering the following criteria. The first criterion is that the maximum voltage at the rotor, V_{r0-max}, during the voltage sag should not exceed $V_{RSC-max}$, the maximum value allowed by the RSC. In other words:

$$V_{RSC-max} \geq V_{r0-max} \tag{12}$$

The second criterion is that during the voltage sag, the sum of the grid-side voltages and the voltage across the SDBR resistor R_{SDBR} should not exceed the maximum value of the stator voltage of the DFIG this means that:

$$V_{s-max} \geq V_{SDBR} + (1-d)V_s \tag{13}$$

$$V_{SDBR} = R_{SDBR} \cdot I_s \tag{14}$$

Where V_{SDBR} is the voltage across resistor R_{SDBR} and V_{s-max} is the maximum stator voltage of the DFIG. From (7)-(9) the maximum rotor voltage can be expressed by (15).

$$V_{r0-max} = \frac{L_m}{L_s}[(1-d)V_s|g| + (1-g)dV_s] \tag{15}$$

If we assume that the voltage $V_d = (1-d)V_s$ is the stator voltage in the event of a voltage dip, (15) becomes (16).

$$V_{r0-max} = \frac{L_m}{L_s}[V_d|g| + (1 - g)(V_s - V_d)] \tag{16}$$

During a voltage dip, the voltage V_d can be expressed in the form of (17).

$$V_d = V_{\text{SDBR}} + (1 - d)V_s \tag{17}$$

Neglecting the rotor losses, the switching losses of the RSC switches, and the ripple effects of the DC bus voltage, the voltage $V_{RSC-max}$ can be written as (18).

$$V_{RSC-max} \approx \frac{V_{dc}}{\sqrt{3}} \tag{18}$$

From (12), (14), (15), (17), and (18), the minimum value of resistance R_{SDBR} is deduced using (19).

$$R_{\text{SDBR}-min} \geq \frac{1}{(1-g-|g|)I_s}\left[(1 - d)V_s|g| + (1 - g)dV_s - \frac{L_s}{L_m}\frac{V_{dc}}{\sqrt{3}}\right] \tag{19}$$

In the same way, and to satisfy the second criterion in (13), the maximum value of the resistance R_{SDBR} is deduced, using (20).

$$R_{\text{SDBR}-max} \leq \frac{V_{s-max}-(1-d)V_s}{I_s} \tag{20}$$

4. RESULTS AND DISCUSSION

A 60% depth symmetrical voltage dip applied for 0.5 seconds to the DFIG is used to investigate the impact of the voltage dip on the system under study and to demonstrate the efficacy of the suggested control solutions (Figure 8). As long as the fault duration is much less than the changes in wind speed, the wind profile is fixed at 10 m/s and is regarded as constant. In this phase of simulation, a comparison between the two methods; crowbar and SDBR will be the object of this part of the simulation to illustrate the improvement that the SDBR technique brings on the general behavior of the DFIG during a fault on the network. The operation of the wind energy conversion chain in the event of a voltage dip is simulated under the MATLAB/Simulink environment with $R_{cw} = 0.37\ \Omega$, $R_{\text{SDBR}} = 0.28\ \Omega$, and $R_{DC} = 0.37\ \Omega$.
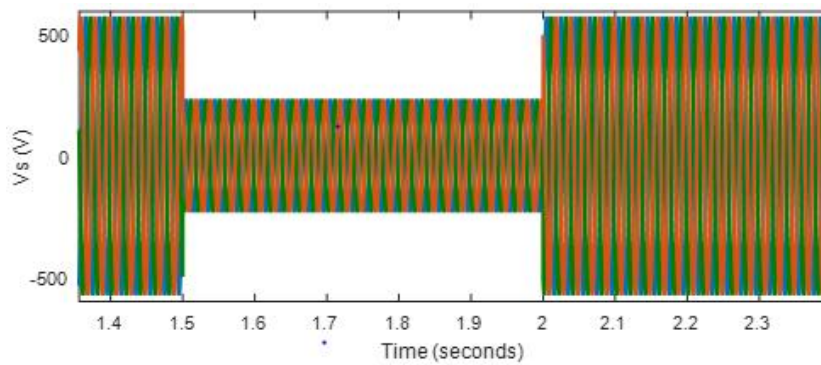

Figure 8. Stator voltage with a 60% voltage dip

The rotor speed profile is illustrated in Figure 9. As a result of the inertial storage of excess power, the rotor speed increases suddenly when a fault occurs. Compared to the crowbar, the SDBR technique has a lower speed deviation because the power transmitted to the grid decreases during the fault while the power captured by the turbine stays constant.

Figure 10 shows the DC bus voltage during the voltage dip. The DC bus voltage rises from 1150 V to 1175 V for the SDBR technique, whereas for the crowbar it rises from 1150 V to 1275 V, which means that the SDBR has a minimum overshoot compared with the crowbar. Thanks to the DC-chopper, the DC bus voltage must never exceed $1.1 * V_{dc}$. When the fault disappears, the DC bus voltage quickly returns to its nominal value, unlike the crowbar circuit.
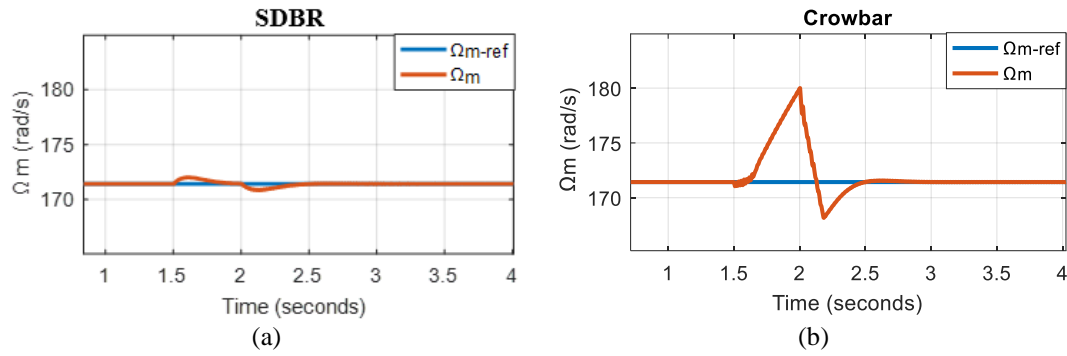
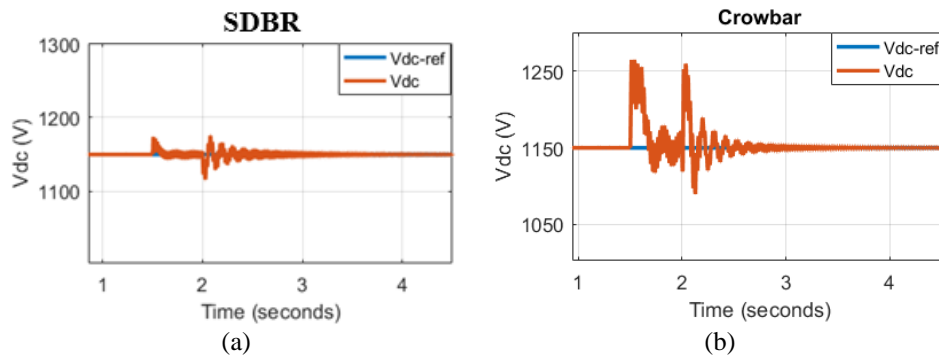Figure 9. Rotor speed profile: (a) SDBR technique and (b) crowbar

Figure 10. DC bus voltage: (a) SDBR technique and (b) crowbar

Figures 11 and 12 show the stator currents and the rotor currents respectively. During the voltage dip period, these currents do not exceed the permitted limits and the peaks in the stator and rotor currents are due to the insertion and removal of the protection device used in either the crowbar circuit or the SDBR technique. Figure 13 shows the evolution of the current circulating in the filter I_f (mains side). One can see that during the fault, these currents increase due to the increase in the DC bus voltage, and when the fault disappears, these currents return to their initial values more quickly for the SDBR, unlike the crowbar circuit.

Figure 14 shows the active stator power during the voltage dip. After the mains voltage dips, the stator power becomes very low. The transfer of power from the stator to the mains resumes once the fault has disappeared and the power returns to its initial value.
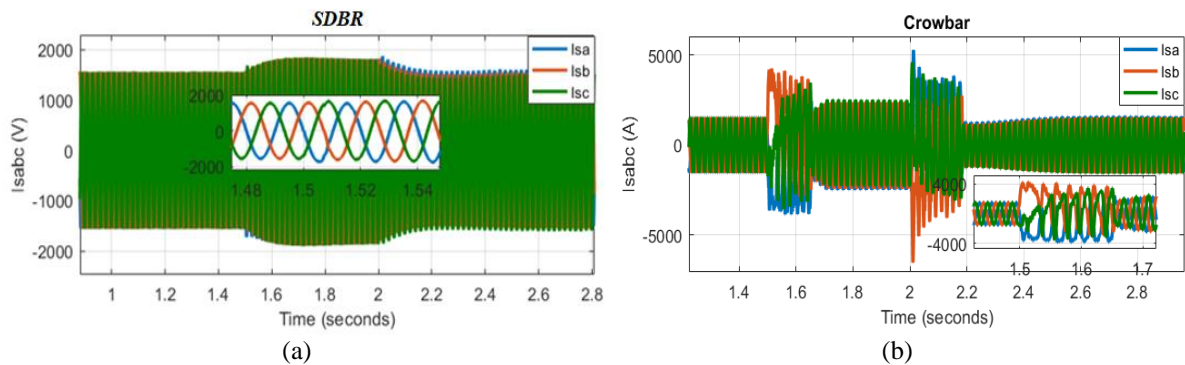

Figure 11. Stator currents during voltage dips: (a) SDBR technique and (b) crowbar
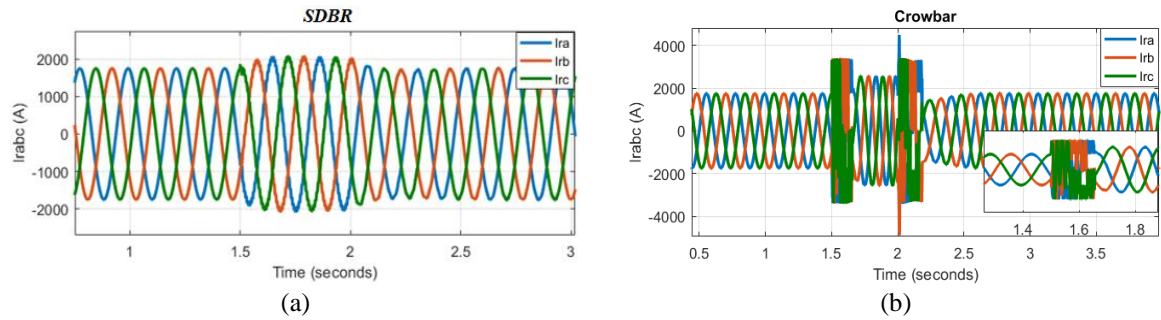
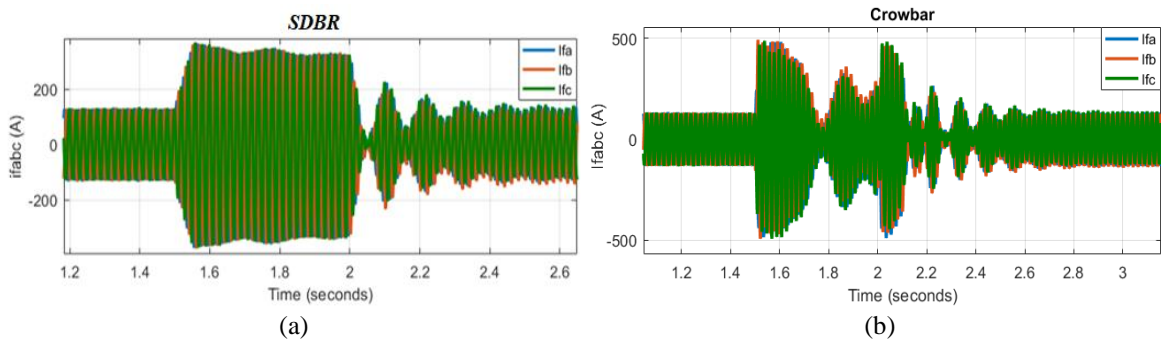Figure 12. Rotor currents during voltage dips: (a) SDBR technique and (b) crowbar

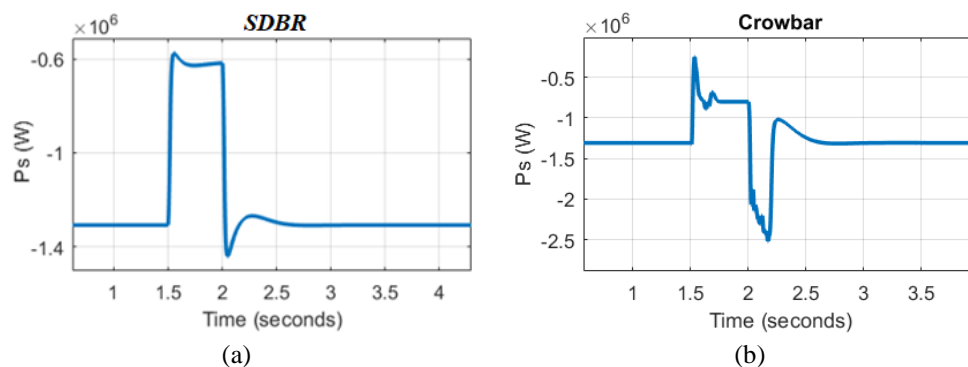Figure 13. Filter current if (a) SDBR technique and (b) crowbar

Figure 14. Stator active power: (a) SDBR technique and (b) crowbar

5. CONCLUSION

In order to enhance the transient stability and LVRT capability of the DFIG during a symmetrical voltage dip, we examined the behavior of the wind system in this study and suggested two distinct methods: crowbar and SDBR. Compared to the crowbar technique, the SDBR technique performs well based on the data obtained. The SDBR technique is more effective in limiting fault currents and improving DFIG performance. Simulation results were presented to show the validity and effectiveness of the control strategy of the two proposed methods, which allow the wind system to remain connected to the grid during the voltage dip and to return to normal operation after the fault has disappeared.

REFERENCES

[1]   C. Chen, A. Bagheri, M. H. J. Bollen, and M. Bongiorno, "The impact of voltage dips to low-voltage-ride-through capacity of doubly fed induction generator based wind turbine," in *2019 IEEE Milan Power Tech*, IEEE, Jun. 2019, pp. 1–6, doi: 10.1109/PTC.2019.8810749.

[2]   M. Fdaili, A. Essadki, I. Kharchouf, and T. Nasser, "Noncontrolled fault current limiter with reactive power support for transient stability improvement of DFIG-based variable speed wind generator during grid faults," *International Transactions on Electrical Energy Systems*, vol. 31, no. 8, Aug. 2021, doi: 10.1002/2050-7038.12955.

[3]   M. Fdaili, T. Nasser, A. Essadki, M. Nadour, and I. Kharchouf, "Control strategies for DFIG-based wind turbine systems contributing to LVRT improvement and grid primary frequency adjustment," in *2020 International Conference on Electrical and Information Technologies (ICEIT)*, IEEE, Mar. 2020, pp. 1–6, doi: 10.1109/ICEIT48248.2020.9113195.

[4]   W. Guo *et al.*, "LVRT capability enhancement of DFIG with switch-type fault current limiter," *IEEE Transactions on Industrial Electronics*, vol. 62, no. 1, pp. 332–342, Jan. 2015, doi: 10.1109/TIE.2014.2326997.

[5]   M. Ezzat, M. Benbouzid, S. M. Muyeen, and L. Harnefors, "Low-voltage ride-through techniques for DFIG-based wind turbines: state-of-the-art review and future trends," in *IECON 2013 - 39th Annual Conference of the IEEE Industrial Electronics Society*, IEEE, Nov. 2013, pp. 7681–7686, doi: 10.1109/IECON.2013.6700413.

[6]   I. Khan *et al.*, "Dynamic modeling and robust controllers design for doubly fed induction generator-based wind turbines under unbalanced grid fault conditions," *Energies (Basel)*, vol. 12, no. 3, p. 454, Jan. 2019, doi: 10.3390/en12030454.

[7]   D. Zhu, X. Zou, L. Deng, Q. Huang, S. Zhou, and Y. Kang, "Inductance-emulating control for DFIG-based wind turbine to ride-through grid faults," *IEEE Transactions on Power Electronics*, vol. 32, no. 11, pp. 8514–8525, Nov. 2017, doi: 10.1109/TPEL.2016.2645791.

[8]   N. Khemiri and A. Khedher, "A comparison of conventional and modified vector control strategies for controlling transient currents and voltage dips in grid-connected wind and photovoltaic hybrid system," *Environmental Progress & Sustainable Energy*, vol. 39, no. 5, Sep. 2020, doi: 10.1002/ep.13415.

[9]   J. Liang and R. G. Harley, "Feed-forward transient compensation control for DFIG wind generators during both balanced and unbalanced grid disturbances," in *2011 IEEE Energy Conversion Congress and Exposition*, IEEE, Sep. 2011, pp. 2389–2396, doi: 10.1109/ECCE.2011.6064086.

[10] B. Babaghorbani, M. T. Hamidi Beheshti, and H. A. Talebi, "An improved model predictive control of low voltage ride through in a permanent magnet synchronous generator in wind turbine systems," *Asian Journal of Control*, vol. 21, no. 4, pp. 1991–2003, Jul. 2019, doi: 10.1002/asjc.2149.

[11] M. Chakib, A. Essadki, and T. Nasser, "A comparative study of PI, RST, and ADRC control strategies of a doubly fed induction generator based wind energy conversion system," *International Journal of Renewable Energy Research*, vol. 8, no. 2, pp. 964–973, 2018, doi: 10.20508/ijrer.v8i2.7645.g7383.

[12] Y. Moumani, A. J. Laafou, A. A. Madi, and R. Boutssaid, "An improved dual vector control for a doubly fed induction generator based wind turbine during asymmetrical voltage dips," *Bulletin of Electrical Engineering and Informatics*, vol. 13, no. 5, pp. 3757–3769, Oct. 2024, doi: 10.11591/eei.v13i5.7969.

[13] A. J. Laafou, A. A. Madi, A. Addaim, and A. Intidam, "Dynamic modeling and improved control of a grid-connected DFIG used in wind energy conversion systems," *Mathematical Problems in Engineering*, vol. 2020, pp. 1–15, Jul. 2020, doi: 10.1155/2020/1651648.

[14] A. J. Laafou, A. A. Madi, Y. Moumani, and A. Addaim, "Proposed robust ADRC control of a DFIG used in wind power production," *Bulletin of Electrical Engineering and Informatics*, vol. 11, no. 3, pp. 1210–1221, Jun. 2022, doi: 10.11591/eei.v11i3.3539.

[15] R. Chakib, A. Essadki, and M. Cherkaoui, "Active disturbance rejection control for wind system based on a DFIG," *World Academy of Science, Engineering and Technology International Journal of Electrical, Computer, Energetic, Electronic and Communication Engineering*, vol. 8, no. 8, 2014.

[16] O. Barambones, "Sliding mode control strategy for wind turbine power maximization," *Energies (Basel)*, vol. 5, no. 7, pp. 2310–2330, Jul. 2012, doi: 10.3390/en5072310.

[17] A. J. Laafou, A. A. Madi, Y. Moumani, and A. Addaim, "Improving LVRT for DFIG used in WPCS under voltage dip," in *2023 3rd International Conference on Innovative Research in Applied Science, Engineering and Technology (IRASET)*, IEEE, May 2023, pp. 01–05, doi: 10.1109/IRASET57153.2023.10152878.

[18] J. López, E. Gubĺa, P. Sanchis, X. Roboam, and L. Marroyo, "Wind turbines based on doubly fed induction generator under asymmetrical voltage dips," *IEEE Transactions on Energy Conversion*, vol. 23, no. 1, pp. 321–330, Mar. 2008, doi: 10.1109/TEC.2007.914317.

[19] M. R. Islam *et al.*, "Fault ride through capability improvement of DFIG based wind farm using nonlinear controller based bridge-type flux coupling non-superconducting fault current limiter," *Energies (Basel)*, vol. 13, no. 7, p. 1696, Apr. 2020, doi: 10.3390/en13071696.

[20] L. Peng, B. Francois, and Y. Li, "Improved crowbar control strategy of DFIG based wind turbines for grid fault ride-through," in *2009 Twenty-Fourth Annual IEEE Applied Power Electronics Conference and Exposition*, IEEE, Feb. 2009, pp. 1932–1938, doi: 10.1109/APEC.2009.4802937.

[21] B. Liu, C. Xu, J. Gui, C. Lin, and M. Shao, "Research on the value of crowbar resistance to low voltage ride through of DFIG," in *2015 International Conference on Computer and Computational Sciences (ICCCS)*, IEEE, Jan. 2015, pp. 44–48, doi: 10.1109/ICCACS.2015.7361320.

[22] Y. Moumani, A. J. Laafou, and A. A. Madi, "Modeling and backstepping control of DFIG used in wind energy conversion system," in *2021 7th International Conference on Optimization and Applications (ICOA)*, IEEE, May 2021, pp. 1–6, doi: 10.1109/ICOA51614.2021.9442625.

[23] A. Moghassemi and S. Padmanaban, "Dynamic voltage restorer (DVR): A comprehensive review of topologies, power converters, control methods, and modified configurations," *Energies (Basel)*, vol. 13, no. 16, p. 4152, Aug. 2020, doi: 10.3390/en13164152.

[24] A. Noubrik, L. Chrifi-Alaoui, P. Bussy, and A. Benchaib, "Analysis and simulation of a crowbar protection for DFIG wind application during power systems disturbances," in *Journal of Mechanics Engineering and Automation*, vol. 3, pp. 303-312, 2011, [Online]. Available: https://api.semanticscholar.org/CorpusID:107293589

[25] H. Soliman, H. Wang, D. Zhou, F. Blaabjerg, and M. I. Marie, "Sizing of the series dynamic breaking resistor in a doubly fed induction generator wind turbine," in *2014 IEEE Energy Conversion Congress and Exposition (ECCE)*, IEEE, Sep. 2014, pp. 1842–1846, doi: 10.1109/ECCE.2014.6953642.

[26] M. S. Alam, M. A. Abido, M. I. Hossain, Md. S. H. Choudhury, and M. A. Uddin, "Series dynamic braking resistor based protection scheme for inverter based distributed generation system," in *2018 International Conference on Innovations in Science, Engineering and Technology (ICISET)*, IEEE, Oct. 2018, pp. 231–235, doi: 10.1109/ICISET.2018.8745629.

[27] M. S. Alam, M. I. Hossain, M. A. Hossain, M. S. H. Choudhory, and M. A. Uddin, "Protection of inverter-based distributed generation with series dynamic braking resistor: a variable duty control approach," in *2018 10th International Conference on Electrical and Computer Engineering (ICECE)*, IEEE, Dec. 2018, pp. 253–256, doi: 10.1109/ICECE.2018.8636781.

BIOGRAPHIES OF AUTHORS

Abdeslam Jabal Laafou was born in Morocco. He received the Ph.D. degree of Electrical Engineering in 2023 from the National School of Applied Sciences, Ibn Tofail University, Kenitra, Morocco. He received the Master degree of Electrical Engineering from the ENSET of Rabat, Mohammed V University, Rabat, Morocco. He is currently a professor of Electrical Engineering. His research interests are control strategies of wind power systems. He can be contacted at email: abdeslam.jaballaafou@uit.ac.ma.

Abdessalam Ait Madi was born in Morocco. He received a teaching engineering degree in electronics from the ENSET of Mohammedia. He received his master's and Ph.D. degrees from the Faculty of Sciences and Technologies from the Sidi Mohamed Ben Abdellah University of Fez in Morocco. He received the Habilitation degree from the Faculty of Sciences of Ibn Tofail University. He is an Associate Professor at the National School of Applied Sciences of Ibn Tofail University in Kenitra, Morocco. He can be contacted at email: abdessalam.aitmadi@uit.ac.ma.

Youssef Moumani received master's degree in Sciences and Technology specialty: Automatic, Signal Processing, and industrial computing in 2014, from the Faculty of Science and Technology, Hassan I University, Settat, Morocco. He is currently a Ph.D. Student at National School of Applied Sciences, Ibn Tofail University, Kenitra Morocco. His research interests are control strategies of wind power systems. He can be contacted at email: youssef.moumani@uit.ac.ma.

Hassan Essakhi received his Ph.D. in Electrical Engineering at the ENSA (National School of Applied Sciences), Ibn Zohr University, Agadir. Teacher of Electrical Engineering, with a bachelor's in electromechanics at Higher Normal School of Technology (ENSET), Mohammadia, Morocco, and a master's degree in Electrical Engineering at the Cadi Ayyad University in Marrakesh, Morocco. His research, in the context of a national doctoral thesis, focuses on the theme of Renewable Energies. The doctoral investigations took place in the Research Team in Engineering Sciences and Energy Management (LASIME) Agadir, Morocco. He can be contacted at email: hassan.essakhi@edu.uiz.ac.ma.